GEOPHYSICAL RESEARCH LETTERS, VOL. 25, NO.14, PAGES 2561-2564, JULY 15, 1998

Energetic electron injections into the inner magnetosphere during the Jan. 10-11, 1997 magnetic storm

Xinlin Li,[1] D. N. Baker,[1] M. Temerin,[2] T. Cayton,[3] G. D. Reeves,[3] T. Araki [4] H. Singer,[5] D. Larson,[2] R. P. Lin,[2] S. G. Kanekal[6]

Abstract. At the end of the main phase of the Jan. 10-11, 1997 magnetic storm, a rapid enhancement of 0.4–1.6 MeV electrons across L=4.2–6 was measured by particle detectors on the Solar, Anomalous, and Magnetospheric Particle Explorer (SAMPEX) and three Global Positioning System (GPS) satellites. This enhancement, over two orders of magnitude at L=4.2–5, occurred around 11:00 UT on Jan. 10, when the AE index reached ~ 2000 nT and when a solar wind pressure pulse arrived. Using data from multiple satellites and ground stations, we determine that the rapid enhancement of 0.4–1.6 MeV electrons in the magnetosphere at L=4.2–6 was due to a combination of intense substorm activity during the early part of the magnetic storm which produced a source population and the following pressure pulse which quickly energized some of these electrons by moving them into stronger magnetic field.

Introduction

Energetic electrons (>0.4 MeV) in the outer radiation belt demonstrate variability on time scales as long as a solar cycle and as short as the passage of a strong interplanetary shock (~ 1 minute). The largest variations of the electron flux are associated with magnetic storms during which the relativistic electron flux typically drops at the beginning of the main phase and starts to recover during the recovery phase, often exceeding pre-storm levels within a couple of days [Baker et al., 1994; Li et al., 1997a; Li et al., 1997b]. The electron flux can also be promptly enhanced by a strong interplanetary shock. A dramatic example is the CRRES event of March 24, 1991 when a strong interplanetary shock struck the magnetosphere generating intense fluxes of both electrons and ions in 90 seconds, such that a new electron and ion radiation belt were formed at L~2.5 in less than one drift period (150 seconds) of the 15 MeV electrons [Vampola and Korth, 1992; Blake et al., 1992]. This earlier event was modeled by using a magnetosonic pulse to achieve agreement between the observed and simulated electron and proton drift echoes [Li et al., 1993; Hudson et al., 1995]. Here, we investigate whether smaller pressure pulses can also produce rapid enhancements of relativistic electrons in the inner magnetosphere by analyzing a solar wind pressure pulse-related enhancement of the outer belt electron flux that occurred at the end of the main phase of the magnetic storm of Jan. 10-11, 1997. We use satellite data from WIND, SAMPEX, the GPS series, and the Los Alamos National Laboratory (LANL) sensors on geosynchronous satellites.

[1]LASP, University of Colorado, Boulder
[2]Space Sciences Lab., University of California, Berkeley
[3]Los Alamos National Lab., Los Alamos, New Mexico
[4]Space Environment Center/NOAA, Boulder, Colorado
[5]Dept. of Geophysics, Kyoto University, Kyoto, Japan
[6]NASA GSFC and Hughes STX, Greenbelt, Maryland

Paper number 98GL00036.
0094-8534/98/98GL-00036$05.00

Observations and Discussion

Figure 1 shows solar wind quantities measured by WIND on Jan. 10, 1997 while WIND was moving from (84.8,-59.6,-3.4) to (93.2,-57.6,-4.5)R_E (Earth radius) in GSE coordinates [Lin et al., 1995; Lepping et al., 1995]. Panel (a) shows the energetic electrons from 27.2 keV to 182 keV. The phase space density of these electrons is smaller than the phase space density of the energetic electrons with the same first adiabatic invariant (μ) in the magnetosphere, ruling out, as was shown before [Li et al., 1997a], that these electrons are the direct source (transported in while conserving μ) of the enhancements in the outer radiation belt. Panel (b)-(d) show the solar wind velocity, density, and dynamic pressure. The velocity did not show large changes. However, the solar wind density and thus the dynamic pressure did, and the most notable changes occurred around 1:00 UT and 10:30 UT. Panels (e)-(g) show the solar wind magnetic field (courtesy of R. Lepping), which was remarkably steady at $B \sim 15$ nT from 5:00 UT to 24:00 UT, while it remained southward at B_z=-(10–15)nT for many hours before slowly turning northward.

We now study the response of the magnetosphere and of the relativistic electrons for these solar wind condi-

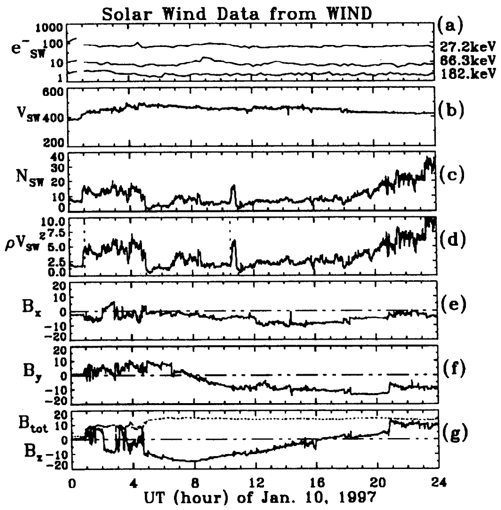

Figure 1. (a) differential flux of electrons (/cm^2-s-sr-MeV) in the solar wind (every 15 min) with the energy ranges labeled on the figure; (b), (c), (d) solar wind velocity, V_{sw}, solar wind plasma density, N_{sw}, and solar wind dynamic pressure, P_{sw}, (every 12.3 s); (e), (f), (g) x, y, and z component (in GSE coordinates) and magnitude (dotted line) of the IMF (every 3 s).

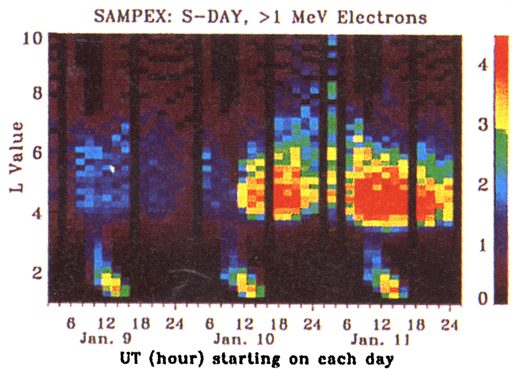

Figure 2. Color-coded electron fluxes from SAMPEX HILT channel (>1 MeV electrons and >4 MeV/nucleon ions) [Klecker et al., 1993]. Only the southern dayside ($\sim$ 15 MLT) passes are plotted. The data are binned in 0.2 L-values and the range $1 \leq L \leq 10$ is shown. Electrons dominate the count rate for $3 \leq L \leq 10$. The time for each column of pixels (covering the whole L-shell) is about 20 minutes, and the time between adjacent columns of pixels is one orbital period ($\sim$ 96 min).

tions. Fig. 2 shows integral fluxes of >1 MeV electrons of Jan. 9-11 from the HILT instrument [Klecker et al., 1993] on SAMPEX, which is in a low altitude polar orbit [Baker et al., 1993]. Only measurements during southern dayside ($\sim$ 15 magnetic local time, MLT) passes are shown in order to make a consistent comparison in time. The daily variations of the flux at low L-shell (L$\sim$ 2) are due to very energetic ions (>4 MeV/nucleon) in the inner belt in the South Atlantic Anomaly region, where the Earth's magnetic field is weaker and thus more particles mirror below the spacecraft. This orbital effect also affects the outer zone, where the instrument responds almost exclusively to >1 MeV electrons. The electron flux had been relatively low until an enhancement across a wide range of L (4-6) occurred around 11:00 UT on Jan. 10. This enhancement coincided with the arrival of a solar wind pressure pulse measured by WIND ((88.5,-58.8,-3.9)R_E, GSE) around 10:30 UT (panel (d) of Fig. 1). Afterwards, the energetic electrons continued to increase throughout the entire outer zone and moved to lower L-shells (< 4) on Jan. 11. Thus the electron flux was high on Jan. 11 before the solar wind magnetic field and dynamic pressure reached exceptionally high values, $\geq$25 nT and $\geq$120 nano Pascal (nP), respectively [Baker et al., 1997].

A more detailed view of the energetic electrons can be seen by combining data from GPS satellites [Drake et al., 1993]. Fig. 3 shows counts per second of electrons in different energy ranges (0.2-0.4, 0.4-0.8, 0.8-1.6, 1.6-3.2 MeV) from three GPS satellites, each represented by a different color (NS24=green, NS33=red, NS39=purple). Each satellite passes through a wide range of L values above its minimum L of $\sim$ 4.2 four times during each orbit. By combining the three satellites one gets an almost continuous record of the energetic electron flux at each L larger than L=4.2. The L values used in presenting the GPS data are calculated using an updated IGRF model for the internal field and a quiet-time Tsyganenko-89 model [Tsyganenko, 1989]. Each L panel here is actually a plot of the count rate within 96-second bins when the GPS satellite is within 0.25-L of the nominal value. The MLT at midnight UT of the three GPS satellites is approximately 12:00 for NS24 (green), 1:30 for NS33 (red), 8:40 for NS39 (purple) and advances roughly two hours for each real hour. We have adjusted for the slightly different background count levels and effective geometric factors of the different GPS satellites and channels to produce a more uniform presentation. Also shown in Fig. 3 is the 5-minute resolution D_{st} index calculated by G. Lu of HAO/NCAR [G. Lu, private comm., 1997].

The top right panel of Fig. 3 (0.8-1.6 MeV) demonstrates, as was shown before in Fig. 2, that there was a sharp enhancement of the electron flux from a low level in the center of the outer zone (L=4–6) at about 11:00 UT on Jan. 10 in coincidence with the arrival of the solar wind pressure pulse measured earlier by WIND near 10:30 UT. This pressure pulse is also indicated by the D_{st} jump around 11:00 UT on Jan. 10.

Before the enhancement, measurable flux levels were low and comparable to the GPS background levels. Right after the enhancement around 11:00 UT on Jan. 10, 0.4-3.2 MeV electrons peaked between L=4.25 and 4.5 and within a few hours moved inward of the GPS satellites' orbits (L=4.2), which is indicated by the negative slope of the flux vs. L at L=4.2 in the plots of the GPS data as a function of L.

The top left panel of Fig. 3 shows that the enhancement of 0.2-0.4 MeV electrons at L=4.25, 4.5, and 5 occurred prior to the jump of D_{st} at 11:00 UT on Jan. 10. This suggests that these lower energy electrons were injected inwards along with the storm ring current ion injection (indicated by the D_{st} decrease). The 0.4-0.8 MeV electrons at L=4.25, 4.5, and 5 increased slightly before the jump in D_{st} around 11:00 UT but the largest increase (NS39-purple) coincided with the D_{st} jump. The 1.6-3.2 MeV channel shows a variation similar to the 0.8-1.6 MeV channel.

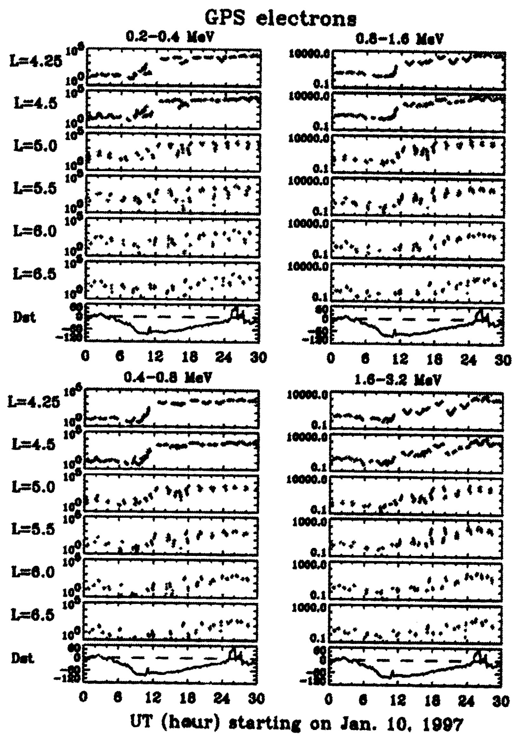

Figure 3. Count rate of electrons at various L-values in various energy ranges from 3 GPS satellites, represented by different colors (NS24=green, NS33=red, NS39=purple). High time resolution (every 5 min) D_{st} (courtesy of G. Lu) is also plotted.

The data show, however, that the earlier pressure pulse around 1:00 UT on Jan. 10, produced no change in the outer radiation belt electrons unlike the one at 11:00 UT which correlated with a two orders of magnitude enhancement of the energetic electrons (>0.4 MeV) at L=4.2-5. In general, a solar wind pressure pulse compresses the magnetosphere producing an induced electric field, roughly pointing westward, which propagates through the magnetosphere. This propagating field can quickly energize electrons that drift around the Earth due to the gradient and curvature of the geomagnetic field. The energy gain of such an electron is sensitive to the electron's initial energy and to its ability to stay in phase with the induced electric field (an electron's drift speed should be comparable to the propagation speed of the electric field) [Li et al., 1993; Li et al., 1996]. Therefore, an adequate pre-existing seed population of electrons at higher L is required for the pressure pulse to be effective in energizing a substantial number of electrons by moving them to lower L (L=4.2–5). Now we address the question of whether these electrons existed prior to 11:00 UT on Jan. 10.

Due to the prolonged southward solar wind magnetic field, geomagnetic activity was intense on Jan. 10. The quick look AE index derived by the World Data Center-C2 for Geomagnetism, Kyoto, reached 400 nT at 4:00 UT, 1000 nT at 7:00 UT, and 2000 nT at 11:00 UT. Fig. 4 shows the dynamic pressure measured by the Comprehensive Plasma Instrument (CPI) onboard Geotail (courtesy of L. Frank) and electron fluxes in the energy range of 150-750 keV from identically-made LANL sensors onboard three geostationary satellites for Jan. 10. Geotail was in the magnetosheath most of the time before 11:15 UT except for three intervals when it was inside magnetopause: prior to 1:00 UT, 5:00-6:00 UT, and 9:30-10:00 UT. So the dynamic pressure measured by Geotail resembles that measured by WIND, panel (d) of Fig. 1, with some propagation time delay.

The LANL sensors measured the first electron and proton (not shown here) injection around 4:30 UT. The electron fluxes with energies <500 keV increased almost simultaneously (as seen in this plotting time scale). The rise time was much shorter than the electron's drift period and drift echoes were clearly observed by all three satellites. By comparing the different arrival times of electrons of different energies, we determined that this injection occurred around 1:00 MLT. A second electron injection, also starting around 1:00 MLT and well measured by the all three satellite, occurred near 7:00 UT. This time 500-750 keV electrons were also seen, and there were subsequent injections right after the initial one, so the would-be drift echoes were mixed up with new injections. During this period, both EISCAT and IRIS data also show enhanced energetic electron precipitations [I. McCrea, private comm., 1997]

Another electron flux enhancement occurred just before 11:00 UT, indicated by the dashed vertical line in Fig. 4. This might be due to a substorm-associated injection. The net result was that the electron flux in the energy range 150-500 keV (satellite 1994-084) was significantly higher at 11:00 UT than at 1:00 UT, and the electron flux in the energy range 150-315 keV (satellite 1991-080) was also higher at 11:00 UT than at 1:00 UT. These electrons could be the source population needed for >0.4 MeV electrons measured by GPS satellites at lower L-shells (Fig. 3). Another difference between these two periods (1:00 UT and 11:00 UT) is in the magnetospheric activity. The AE index had been less than 20 nT for many hours prior to 1:00 UT but reached 2000 nT at 11:00 UT. The pressure pulse around 11:00 UT arrived after many hours of sustained southward solar wind magnetic field and intense substorm activity. These factors could have contributed to the rapid injection of > 0.4 MeV electrons into the inner magnetosphere at 11:00 UT but not at 1:00 UT. The question still remains if the observed >0.4 MeV electron enhancement at L< 5 (Fig. 3) is simply due to intense substorm activity or due to a combination of intense substorm activity and the solar wind pressure pulse. Note that during the first two substorm injections, 4:30 UT and 7:00 UT, there was no >0.4 MeV electron enhancements at L< 5 discernible by GPS. (Nor did the GPS satellites, perhaps because they are then farther from the equatorial plane, measure any significant enhancement of >0.4 MeV electrons around 4:30 UT or 7:00 UT at larger L shells.)

Figure 5 shows the 10:30–11:00 UT period in greater detail: (a) the solar wind dynamic pressure measured by WIND; (b) the dynamic pressure measured by Geotail;

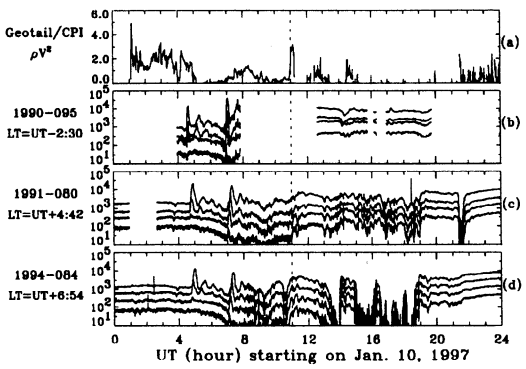

Figure 4. (a) dynamic pressure measured (1 min resolution) by Geotail/CPI (courtesy of L. Frank), (b), (c), (d) pitch angle-averaged electron differential flux (/s-sr-cm^2-keV) in the energy ranges of 150-225 keV, 225-315 keV, 315-500 keV, and 500-750 keV (from top to bottom in each of the three panels) from LANL sensors onboard three geostationary satellites (10 s resolution).

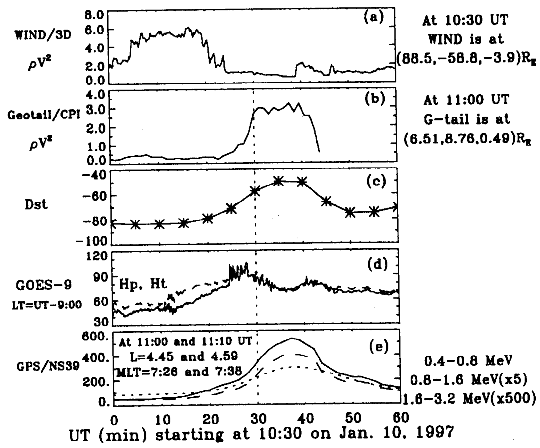

Figure 5. (a) solar wind dynamic pressure (every 12.3 sec), (b) dynamic pressure measured (every 1 min) by the Geotail/CPI, (c) high time resolution (every 5 min) D_{st} , (d) parallel (to Earth's spin axis) component, H_p, and magnitude, H_t of magnetic field measured (every 0.5 sec) at GOES-9, (e) electron count rate (every 96 sec) from one GPS satellite (NS39).

(c) D_{st} ; (d) the magnetic field measured by GOES-9; and (e) the electron count rate from one GPS satellite, the count rate for 0.8-1.6 MeV (dashed line) and 1.6-3.2 MeV (dotted) has been multiplied by a factor of 5 and 500, respectively. The magnetic field at GOES-9 increased sharply right after 10:54 UT, and individual ground stations at different longitudes that are used to calculate the D_{st} value all show a jump in the H-component of the magnetic field around the same time. These features suggest a global compression, which is consistent with the enhancement of the dynamic pressure measured by Geotail. However, the exact timing of the compression may be more accurately indicated by the magnetometer data from both ground stations and from GOES-9, since Geotail was in the magnetosheath where the bulk flow of the plasma varies greatly from place to place. The electron count rates from various channels (panel (e)) show the rapid enhancement following the arrival of the pressure pulse (panel (b)), on a time scale of 10 minutes, which is shorter than the drift period of 0.8 MeV electron at L=4.5 (18 minutes) and therefore indicates the third adiabatic invariant of the electron was violated. Substorm activity had been strong even before 10:54 UT on Jan. 10, as suggested by the high AE index and the particle injections at geostationary orbit, but there was no enhancement of 0.4–1.6 MeV electrons around L=4.4 until the pressure pulse arrived, which is also represented by the D_{st} rise. This suggests that the pressure pulse was responsible for the rapid enhancement of the 0.4–1.6 MeV electrons at L=4.2-6 measured by the GPS satellites.

If we fit the GPS measurement of 0.2–1.6 MeV electrons with a power law, we get a power index of -3.77. We found, using T-95 model [N. Tsyganenko, private comm., 1995] plus dipole field and the added magnetic field from the pulse (23 nT based on ground observations), that a 0.8 MeV electron at L=4.5 coming from L=6 while conserving μ would have started with an initial energy 0.36 MeV. If the electron comes from farther away, the required initial energy is smaller, and vice versa. We also note that there was enough source population for the observed 0.8 MeV electrons at L=4.5 since the phase space density of 0.36 MeV electrons at L=6 as measured by the GPS satellites before the pressure pulse was 33% greater than that of the later measured 0.8 MeV electrons at L=4.5, even assuming an isotropic pitch angle distribution.

Summary and Conclusions

We have shown a rapid enhancement of 0.4–1.6 MeV electrons in the magnetosphere at L=4.2–6, which occurred after a long period of steady southward interplanetary magnetic field (IMF) and followed the arrival of a solar wind pressure pulse. We argue that strong substorm activity, as a result of the prolonged southward IMF prior to the pressure pulse, produced the source electrons in the energy range of tens of keV to hundreds of keV near or inside geostationary orbit. The subsequent solar wind pressure pulse further energized some of these electrons and transported them inward on a time scale of 10 minutes. Had there been no pressure pulse, the relativistic electrons in the inner magnetosphere would still likely have increased due to strong storm or substorm activity, but the enhancement would have occurred more slowly.

Though it may be possible for rapid changes in the electron flux to be produced by electric fields associated with intervals of bursty convection within the inner magnetosphere or by large scale induction electric fields from intense dipolarizations, which have been observed during some active geomagnetic times [J. Wygant, private comm., 1997], however, these electric fields are not associated with a global compression of the magnetic field, as reflected by a sharp jump of the H-component of the magnetic field measured by ground stations at different longitudes. We conclude that the rapid enhancement of 0.4–1.6 MeV electrons in the magnetosphere at L=4.2–6 was due to a combination of intense substorm activity during the early part of the magnetic storm which produced a source population of somewhat less energetic electrons and the following pressure pulse which quickly energized some of these electrons by moving them into stronger magnetic field.

Acknowledgments. We thank L. Frank, R. Lepping, and G. Lu for providing Geotail plasma pressure data, WIND magnetic field data, and the high resolution D_{st} data, respectively. Special thanks are extended to B. Kleker et al. who were responsible for SAMPEX/HILT instrument development. We also thank J. B. Blake for useful discussions regarding the EISCAT and IRIS observations. Programming effort by Steve Monk is acknowledged. The work at University of Colorado was supported by NASA grant NAG5-4896, NAG5-2681, and NSF grant ATM-9624390.

References

Baker, D. N. et al., An overview of the Solar Anomalous and Magnetospheric Particle Explorer (SAMPEX) mission, *IEEE Trans. on Geosci. and Remote Sensing, 31*, 531, 1993.

Baker, D. N. et al., Relativistic electron acceleration and decay time scales in the inner and outer radiation belts: SAMPEX, *Geophys. Res. Lett.*, *21*, 409, 1994.

Baker, D. N. et al., Coronal Mass Ejections, Magnetic Clouds, and Relativistic Magnetospheric Electron Event: ISTP, *J. Geophys. Res.*, in press, 1998.

Blake J. B. et al., Injection of electrons and protons with energies of tens of MeV into L<3 on March 24, 1991, *Geophys. Res. Lett.*, *19*, 821, 1992.

Drake, D. M. et al, Experimental Evaluation of the BDD-I Dosimeter for the GPS, Nuclear Instruments and Methods in Physics Research, A333, 571, 1993.

Hudson, M. K. et al., Simulation of proton radiation belt formation during the March 24, 1991 SSC, *Geophys. Res. Lett.*, *22*, 291, 1995.

Lepping, R. P. et al., The WIND magnetic field investigation, *Space Science Rev.*, *71*, 207, 1995.

Klecker, B. et al., HILT: A heavy ion large area proportional counter telescope for solar and anomalous cosmic rays, IEEE Trans. Geosci. Rem. Sensing, *31*, 542, 1993.

Li, X. et al., Are energetic electrons in the solar wind the source of the outer radiation belt? *Geophys. Res. Lett.*, *24*, 923, 1997a.

Li, X. et al., Multi-Satellite Observations of the Outer Zone Electron Variation During the 3-4 November 1993 Magnetic Storm, *J. Geophys. Res.*, *102*, 14123, 1997b.

Li, X. et al., Observation and Simulation of the Rapid Formation of a New Electron Radiation Belt During March 24, 1991 SSC, *AIP Conference Proceedings, 383*, edited by G. D. Reeves, 109-117, 1996.

Li, X., I. Roth, M. Temerin, J. Wygant, M. K. Hudson, and J. B. Blake, Simulation of the prompt energization and transport of radiation particles during the March 23, 1991 SSC, *Geophys. Res. Lett.*, *20*, 2423, 1993

Lin, R. P. et al., A three-dimensional plasma and energetic particle investigation for the WIND spacecraft, *Space Science Rev.*, *71*, 125, 1995.

Tsyganenko, N., A magnetic field model with a warped tail current sheet, *Planet. Spa. Sci.*, *37*, 5, 1989.

Vampola A. L. and A. Korth, Electron drift echoes in the inner magnetosphere, *Geophys. Res. Lett.*, *19*, 625, 1992.

D. N. Baker and X. Li, LASP/CU, 1234 Innovation Dr., Boulder, CO 80303-7814; e-mail: lix@kitron.colorado.edu

D. Larson, R. P. Lin, and M. Temerin, SSL, University of California, Berkeley, CA 94720

Tom Cayton and G. D. Reeves, Mail Stop D-436, Los Alamos National Laboratory, Los Alamos, NM 87545

T. Araki, Kyoto University, Kyoto 606, Japan

H. Singer, SEC, 325 Broadway, Boulder, CO 80303

S. G. Kanekal, NASA/GSFC, Greenbelt, MD 20771

(Received October 15, 1997; revised December 8,1997; accepted December 16, 1997.)